Published in final edited form as:
Invest Ophthalmol Vis Sci. 2008 June ; 49(6): 2495–2505. doi:10.1167/iovs.07-0903.

Effects of Modifiers of Glycosaminoglycan Biosynthesis on Outflow Facility in Perfusion Culture

Kate E. Keller, **John M. Bradley**, **Mary J. Kelley**, and **Ted S. Acott**
From the Casey Eye Institute, Oregon Health & Science University, Portland, Oregon.

Abstract

Purpose—Glycosaminoglycans (GAGs) have been implicated in the regulation of outflow resistance of aqueous humor flow through the trabecular meshwork (TM). Their role was further investigated by assessment of the effects of chlorate, an inhibitor of sulfation, and *β*-xyloside, which provides a competitive nucleation point for addition of disaccharide units, in anterior segment perfusion culture.

Methods—Outflow facility was measured in perfused porcine and human anterior organ cultures treated with 20 or 50 mM sodium chlorate, or 1 mM *β*-xyloside. Perturbation of extracellular matrix (ECM) components was assessed in paraffin-embedded sections by immunofluorescence and confocal microscopy. Parallel experiments were conducted on cultured TM cells.

Results—Outflow facility increased in porcine eyes with chlorate (3-fold) and *β*-xyloside (3.5-fold) treatments. In human eyes, outflow increased approximately 1.5-fold and took longer (>48 hours) to occur. By confocal microscopy, immunostaining for chondroitin and heparan sulfates was observed on edges of human TM beams in nontreated eyes, with intense staining in the juxtacanalicular tissue (JCT) region. In treated eyes, staining of beam edges was severely reduced and was instead found in plaques. Chlorate treatment resulted in a striated pattern of GAG staining in the human JCT region. Fibronectin immunostaining was altered in *β*-xyloside-treated eyes, whereas in cell culture, chlorate induced formation of thick fibronectin fibrils, to which tenascin C colocalized.

Conclusions—Disrupting GAG chain biosynthesis increased outflow facility in perfusion culture and induced atypical ECM molecule interactions in cell culture. This study provides direct evidence of the critical role of GAG chains in regulating outflow resistance in human TM.

Glycosaminoglycans (GAGs) are long, linear sugar chains composed of repeating disaccharide units (Fig. 1A).[1,2] There are five main types of GAGs: chondroitin sulfate (CS), dermatan sulfate (DS), heparin/heparan sulfate (HS), keratan sulfate (KS), and hyaluronic acid (HA), which vary, depending on the identity of their disaccharide units. All GAGs, except HA, are sulfated in various positions and to various degrees. For instance, CS chains are commonly sulfated at the 4- and/or 6-hydroxyl positions, DS chains undergo 4- and 2-O-sulfation, whereas HS chains can be N-, 2-O-, 6-O-, and/or 3-O-sulfated.[3,4] All GAG chains, again with the exception of HA, are covalently attached to and synthesized on core proteins to form proteoglycans as they move through the endoplasmic reticulum and Golgi apparatus.[5] These are then integrated into the extracellular matrix (ECM) where they perform many functions, including cell–matrix interactions, growth factor binding and sequestration and maintenance of tissue structural integrity.[1,6]

Corresponding author: Ted S. Acott, Casey Eye Institute, Oregon Health & Science University, 3375 SW Terwilliger Boulevard, Portland, OR, 97239-4197; E-mail: acott@ohsu.edu.

Disclosure: K.E. Keller, None; J.M. Bradley, None; M.J. Kelley, None; T.S. Acott, None

GAG chains are thought to be a major source of resistance to aqueous humor outflow in most mammalian species, although their role in primate eyes remains somewhat controversial.[7–9] The most likely site of outflow resistance resides in the cribriform or juxtacanalicular tissue (JCT) region of the TM, the region that lies immediately adjacent to Schlemm's canal.[10] In primary open-angle glaucoma (POAG), there is increased resistance to aqueous outflow, which results in increased intraocular pressure (IOP).[11] During aging of normal human eyes, there is a progressive loss of sulfated and nonsulfated GAG chains from the TM.[9] In POAG eyes, there is loss of HA, but a concomitant increase in CS chains in the JCT region.[7,12] To study the role of GAGs in TM, anterior segments have been treated with several enzymes, GAGases, which selectively degrade one or more GAGs. Perfusion with hyaluronidase increased outflow facility in numerous animal models, including dogs, cows, rabbits, and rhesus monkeys.[13–17] Chondroitinase ABC was reported to increase outflow facility in bovine and cynomolgus monkey eyes,[18,19] but another study did not show any effects on outflow resistance from acute or chronic injection of chondroitinase ABC into cynomolgus monkey eyes.[20] Differences between these studies have been attributed to variations in the type, purity, and source of enzyme; interspecies differences; or incomplete digestion of GAG chains due to varying enzymatic conditions. Apart from one study that suggested heparitinase increased outflow facility in human eyes (Johnson DH et al. *IOVS* 1999;40:ARVO Abstract 504), similar studies using GAGases on human eyes have proved inconclusive.[21–23]

To investigate the role of GAGs in outflow facility, we observed the effects of two modifiers of GAG biosynthesis. The effects of sodium chlorate, a potent inhibitor of GAG chain sulfation, were analyzed (Fig. 1C).[24] GAGs are normally sulfated through the transfer of a sulfate group from 3′-phos-phoadenosine 5′-phosphosulfate (PAPS).[25] Chlorate inhibits the formation of PAPS by directly competing with sulfate ions.[26] Sulfation of GAGs is developmentally regulated and is important for a number of cellular functions, including growth factor sequestration, cell proliferation, and activating protein ligands.[27,28] In addition, the effects of *p*-nitrophenyl-*β*-D-xylopyranoside (*β*-xyloside) were assessed.[29] *β*-xyloside provides a competitive nucleation point to which disaccharide units are added, thereby inhibiting elongation of endogenous GAG chains on proteoglycan core proteins (Fig. 1B). Perturbation with *β*-xyloside permits investigation of proteoglycan GAG chain function in tissues to be elucidated.[30]

In the present study, the effects of sodium chlorate and *β*-xyloside treatments were assessed in porcine and human anterior segment perfusion organ culture and in TM cells in culture. Changes in the distribution of chondroitin-4-sulfate (C4S), chondroitin-6-sulfate (C6S), HS and HA, were assessed using specific antibodies and confocal microscopy. Since fibronectin has been found to increase expression in TGF-*β*2 perfused porcine eyes[31] and both fibronectin and tenascin C mRNAs are modulated by mechanical stretching of TM cells in culture,[32,33] the distribution of fibronectin and tenascin C were also investigated.

Materials and Methods

Human donor eye pairs were acquired from Oregon Lions Eye Bank (Portland, OR). Average age was 80.1 ± 11.6 years (Table 1). Only eyes without a history of glaucoma were used. Porcine eyes were acquired from Carlton Packing (Carlton, OR); sodium chlorate, *p*-nitrophenyl-*β*-D-xylopyranoside (*β*-xyloside), *p*-nitrophenyl-*α*-D-xylopyranoside (*α*-xyloside), and chondroitinase ABC from Sigma-Aldrich (St. Louis, MO); mouse anti-chondroitin-4-sulfate, mouse anti-chondroitin-6-sulfate, mouse anti-heparan sulfate, and rabbit anti-tenascin C from Chemicon (Temecula, CA); rabbit anti-fibronectin from ABR Bioreagents (Golden, CO); mouse anti-fibronectin from BD-Transduction Laboratories (Franklin Lakes, NJ); hyaluronic acid binding protein from Calbiochem (San Diego, CA); and all AlexaFluor–conjugated secondary antibodies and the viability–cytotoxicity kit for mammalian cells from

Invitrogen-Molecular Probes (Eugene, OR). Draq5 was obtained from Axxora (San Diego, CA); normal goat serum, mounting medium (Fluoromount G), and chamber slides (Labtek II) from Fisher Scientific (Pittsburgh, PA); chondroitinase ABC protease-free (from *Proteus vulgaris*) and heparitinase (from *Flavobacterium heparinum*) from Seikagaku Corp. (Tokyo, Japan); hyaluronidase (from *Streptomyces hyalurolyticus*) from ICN Biomedicals (Aurora, OH); Dulbecco's modified Eagle's medium (DMEM) and penicillin-streptomycin-amphotericin B from Invitrogen (Carlsbad, CA); fetal bovine serum (FBS) from HyClone (Logan, UT); protein markers (Precision Plus) from Bio-Rad (Hercules, CA); and anti-rabbit secondary antibody (IRDye680) from Licor Biosciences (Lincoln, NE).

Perfusion Culture

For perfusion culture, human and porcine eyes were prepared as described previously.[34–36] The globes were bisected, and the iris, aqueous humor, ciliary body, and lens were removed. Human anterior segments containing the cornea, TM and a 15-mm rim of sclera were placed in stationary organ culture in serum-free DMEM for 5 to 7 days, to allow recovery of cells postmortem. This recovery step was omitted for the porcine eyes, as these were dissected within 3 hours of death. For human eyes, time of death to stationary organ culture was not more than 48 hours. Anterior segments were then clamped into a perfusion apparatus and serum-free DMEM was perfused at a constant pressure of 8.8 mm Hg, giving an average flow rate of 1 to 7 μL/min for humans or 2 to 8 μL/min for porcine eyes. These rates are similar to normal physiological rates and pressures found in vivo. Eyes that could not be stabilized at these flow rates were discarded. Table 1 summarizes donor information and flow rate data for human eyes.

Stock solutions of sodium chlorate ($NaClO_3$; ×100) were dissolved in phosphate buffered saline (PBS), while α- and β-xylosides were dissolved in methanol (×1000). After 24 to 48 hours of stable flow rates, serum-free media containing a final concentration of 20 or 50 mM $NaClO_3$,[26] or 1 mM α- or β-xyloside,[29] or vehicle, were added to the flow medium for the times indicated in the figures. For human eyes, one eye of a pair was treated, and the other served as a non-treated control. For experiments investigating the effects of GAGases, media in the flow chamber was exchanged with 2 mL of chondroitinase ABC (0.25 U/mL; Seikagaku),[20] heparitinase (0.01 U/mL)[9] or hyaluronidase (10 U/mL),[17] individually or a combination of all three, in DMEM containing 0.1% bovine serum albumin (BSA). Control eyes were treated with 0.1% BSA in DMEM.

We plotted outflow rates as time (hours) versus normalized flow rate. To calculate "normalized flow rate," we divided actual flow rates by the average flow rate before the start of treatment.[31,36] We then combined data from each experiment, averaged them, and calculated a standard error. Time point "0" represents the start of treatment. The number of eyes used for each treatment is noted in each legend or the text accompanying the figure. Facility data are also presented as normalized flow rate before and at the end of treatment. A Student's *t*-test or a Mann-Whitney ranked sum test was performed to determine significance. A Mann-Whitney ranked sum test was also performed for paired human eyes. $P < 0.05$ was considered significant.

Sectioning and Immunostaining

After treatment, the anterior segments were removed from the flow chambers, and a small wedge was taken from the anterior segment for evaluation by live–dead staining with a viability–cytotoxicity kit for mammalian cells. The remaining tissue was then immediately fixed in 10% neutral-buffered formalin for at least 24 hours. The tissues were decalcified overnight using decalcifying solution (Fisher Scientific) to allow easier sectioning through the sclera. The eyes were cut into approximately 8 to 10 wedges, each of which was embedded in a single paraffin block. Five-micrometer serial radial sections were then cut approximately

perpendicular to Schlemm's canal at the pathology–histology core facility of OHSU cancer center (Oregon Health & Science University). Each paraffin-embedded section therefore contained tissue from 8 to 10 regions around the eye. Hematoxylin and eosin (H&E)–stained slides from several quadrants from each eye were examined to ensure the presence of cells and to evaluate tissue structural organization (data not shown). At least three eyes per treatment were analyzed.

After deparaffinization and hydration, immunostaining was performed. Some tissue sections were predigested with chondroitinase ABC (0.2 U/mL in PBS; Sigma-Aldrich)[37] for 30 minutes at room temperature to allow reactivity of the CS GAG chain antibodies. All slides were blocked with 2% normal goat serum in PBS before addition of primary antibodies diluted in PBS, which were incubated for 3 hours at room temperature. Primary antibodies used were as follows: mouse anti-C4S (1:100), mouse anti-C6S (1:100), mouse anti-heparan sulfate (1:100), rabbit anti-fibronectin (1:500), or biotinylated HA-binding protein (1:100). Negative control experiments with no primary antibody were also performed. After three 5-minute washes with PBS, secondary antibody diluted 1:500 in PBS was added to each well. The secondary antibodies were as follows: AlexaFluor 488–conjugated goat anti-mouse, AlexaFluor 594–conjugated goat anti-rabbit, and AlexaFluor 488–conjugated streptavidin. After incubation at room temperature for 1 hour, the slides were washed in PBS (3 × 5 minutes), and coverslips were mounted (Fluoromount G; Fisher Scientific). Each slide was examined by immunofluorescence and confocal microscopy. At least five sections were evaluated for each antibody by immunofluorescence. For human eyes, a concerted effort was made to show paired images from treated and nontreated eyes from the same individual (e.g., Figs. 6A and 6B, 6D and 6E, 6G and 6H, and 6J and 6K are 20-mM chlorate-treated or nontreated eyes from the same donor).

Immunofluorescence and Confocal Microscopy

Immunostained tissue sections and chamber slides were visualized with differential interference contrast optics on a fluorescence microscope (model BX51; Olympus, Lake Success, NY) equipped with a digital camera (model DC500; Leica, Deerfield, IL). Confocal microscopy was performed with a laser scanning confocal imaging system (1024 ES; Bio-Rad) attached to an inverted microscope (Eclipse TE300; Nikon, Tokyo, Japan). Exposure times and laser settings were determined for control sections, and these settings were then maintained for each treated section. Eye sections were tracked throughout the experiment by using the unique identifying numbers assigned by the eye bank, and therefore treatments were masked until postimage analysis. Confocal images were processed with ImageJ software (available by ftp at zippy.nimh.nih.gov/ or at http://rsb.info.nih.gov/nih-image; developed by Wayne Rasband, National Institutes of Health, Bethesda, MD).

Immunofluorescence of TM Cells in Culture

Human (HTM) or porcine (PTM) TM cells were cultured in DMEM containing 10% FBS and 1% penicillin-streptomycin-amphotericin B, as previously described.[33,36,38–40] Cells between passages 3 and 5 were used in all subsequent experiments. For immunofluorescence, TM cells were plated at high density into four-well chamber slides (Labtek II; Fisher Scientific) and incubated with 20 or 50 mM sodium chlorate or 1 mM β-xyloside, in serum-containing DMEM for 72 hours. After treatment, confluent cells in each four-well slide were fixed in 4% paraformaldehyde in PBS for 5 minutes. All slides were blocked and immunostained as above. Primary antibodies were mouse anti-fibronectin (1: 100) and rabbit anti-tenascin C (1:100). Draq5, a DNA binding dye, was added to the secondary antibody mixture at a dilution of 1:500. Randomly selected fields from each well were imaged by confocal microscopy.

Results

GAG Modifier Effects on Outflow Facility in Porcine Eyes

The effects of *β*-xyloside and sodium chlorate on outflow facility were assessed in porcine anterior segment perfusion cultures (Fig. 2A). *β*-Xyloside treatment increased outflow facility approximately 3.5-fold within 4 hours of treatment compared to the control *α*-xyloside isomer. The increased flow rate was maintained for up to 64 hours. Treatment with 20 mM sodium chlorate increased outflow facility approximately 2.5-fold in 24 hours and to approximately 3-fold by 48 hours, a flow rate that was maintained for up to 64 hours. Conversely, treatment with 50 mM sodium chlorate slightly decreased outflow compared with control eyes. Statistical analysis showed a significant difference between pre- and posttreatment flow rates for 20 mM chlorate- and *β*-xyloside-treated eyes (Fig. 2B). The increase in outflow produced by 20 mM chlorate treatment was reversible by addition of 10 mM sodium sulfate to the medium (Fig. 2C).

Distributions of C4S and C6S were investigated in porcine TM after perfusion culture (Fig. 3). In control eyes, C4S was found to stain intensely throughout the TM (Fig. 3A). Both 20 mM chlorate and *β*-xyloside treatments disrupted the pattern of C4S immunolabeling. Immunostaining in *β*-xyloside-treated eyes (Fig. 3C) seemed to be more fibrillar in nature and was arranged in cablelike structures. In chlorate-treated eyes (Fig. 3B), there was an appearance of unraveling of the cables leaving “frayed” edges. In nontreated porcine eyes, C6S staining was generally found to be cell associated, with some staining at beam edges (Fig. 3D). In 20 mM chlorate (Fig. 3E)- and *β*-xyloside (Fig. 3F)-treated eyes, staining was not found cellularly and that around beam edges was disrupted. The appearance of GAG chain cables and fraying was not observed with C6S staining.

Next, the effects of enzymes that specifically degrade GAG chains were assessed in porcine anterior segment perfusion culture, either individually or in combination (Fig. 4A). Chondroitinase ABC, which degrades CS and DS GAG chains, increased outflow facility 2.3-fold within 5 hours of treatment, and the flow rate was further increased to 3-fold by 24 hours. When porcine anterior segments were treated with heparitinase or hyaluronidase, initial outflow facility was modestly affected (1.75-fold and 1.7-fold increases respectively at 5 hours), but this change in outflow was not sustained and by 24 hours, outflow was not significantly different from the BSA control. When chondroitinase ABC, heparitinase, and hyaluronidase were applied in combination, outflow facility increased by 3-fold within 2 hours and was further increased to 3.9-fold at 24 hours. Comparison of pre- and posttreatment flow rates showed a statistically significant difference in eyes treated with chondroitinase ABC or with a combination of all three enzymes (Fig. 4B).

GAG Modifier Effects on Outflow Facility in Human Eyes

Human donor eyes were also assessed for their ability to respond to sodium chlorate or *β*-xyloside treatment in anterior segment perfusion culture (Fig. 5A). All treatments increased outflow facility, but the magnitude of response was lower than that in porcine eyes, and the effect took longer to occur. At 48 hours, only *β*-xyloside treatment produced significant increases (1.3-fold) compared with control eyes. By 110 hours, all treatments caused significant increases compared with their pretreatment flow rates (Fig. 5B; 1.2-fold for 20 mM chlorate, 1.5-fold for 50 mM chlorate, and 1.6-fold for *β*-xyloside). Again, the observed increase in outflow produced by 20 mM chlorate treatment was reversed by sodium sulfate (Fig. 5C). Flow rates did not return to their pretreatment levels in the time observed, which was also observed for porcine eyes. Again, the response time for the reversal took longer than that of porcine eyes.

Levels and distribution of GAG chains were assessed by immunohistochemistry in human tissue after perfusion culture (Fig. 6). In nontreated control eyes, the patterns of C4S and C6S immunostaining were similar, and they each labeled a thin, apparently pericellular strip around the edge of each TM beam (Figs. 6A, 6D). In addition, there was extensive staining in the JCT region (arrowheads) and there was staining at the center of each beam, in a patchlike dotted-line pattern, which was more prominent in C4S-stained sections. Eyes perfused with chlorate or *β*-xyloside showed a major disruption of CS GAG chain staining. In treated eyes, staining around the beam edges became discontinuous or was highly diminished, and immunostaining at the center of the beams was gone. Instead, staining was found in large, amorphous plaques and in punctate dots throughout the TM. In the JCT of the chlorate-treated eyes (Figs. 6B, 6E), C4S and C6S stained in a more striated pattern than in the control eyes. Treatment with *β*-xyloside also reduced the amount of C4S and C6S immunostaining, but the striated pattern was not observed in the JCT (Figs. 6C, 6F).

Distributions of HS immunostaining (Figs. 6G–I) and HA, detected by HA-binding protein (HAbp; Figs. 6J–L), were also investigated. In control eyes, HS staining was generally similar to CS staining. There was a thin strip of staining around each beam and extensive staining in the JCT region (Fig. 6G). Chlorate (Fig. 6H) or *β*-xyloside treatment (Fig. 6I) disrupted the pattern of HS immunolabeling. Immunostaining again appeared in plaques and punctate dots throughout the tissue, although the plaques were not as apparent as in CS-stained tissue. HAbp intensely stained the JCT region in the control eyes (Fig. 6J), with some staining around the edges of the TM beams closest to the JCT. In 20-mM chlorate-treated eyes (Fig. 6K), HAbp staining was severely reduced, especially in the JCT region, whereas it was completely gone in *β*-xyloside-treated eyes (Fig. 6L). Human eyes treated with 50 mM chlorate had staining patterns for C4S, C6S, HS, and HAbp similar to that described for 20-mM chlorate-treated eyes (data not shown).

Expression of Fibronectin in *β*-Xyloside-Treated Eyes

The distribution of fibronectin was investigated in nontreated and *β*-xyloside-treated human (Figs. 7A, 7B) and porcine (Figs. 7C, 7D) eyes. In control eyes, fibronectin was generally distributed in a uniform, but somewhat patchy, pattern throughout the TM (Figs. 7A, 7C). There was some preferential staining of the TM beams on the inner and outer edges in human eyes. However, in *β*-xyloside-treated eyes, much of the fibronectin staining was lost from the center of the beams and JCT region, leaving sharp lines of immunostaining at the inner and outer edges of some of the TM beams (Figs. 7B, 7D). This pattern was observed in both human and porcine *β*-xyloside-treated eyes. In humans, scattered plaques of staining were also observed in treated eyes, resembling that observed for the CS antibodies.

Expression of Fibronectin and Tenascin C in TM Cell Culture

Expression and deposition of fibronectin and tenascin C in cultured human TM cells was also investigated (Fig. 8). In nontreated control cells, fibronectin (green) assembled into an extensive network composed predominantly of fine fibrils (Fig. 8A). Tenascin C (red) was observed in fibril-like patterns and also in discrete patches (Fig. 8B). Double immunostaining experiments showed that although fibronectin and tenascin C showed some colocalization (yellow), their fibrils were not generally coincident (Fig. 8C). Treatment with 50 mM sodium chlorate decreased the amount of fine fibrillar fibronectin staining and instead, thicker fibrils predominated (Fig. 8D). Tenascin C was assembled into intensely stained thick fibrils, with a reduced amount of background red staining (Fig. 8E). Colocalization showed that tenascin C became preferentially colocalized to thick fibronectin fibrils in chlorate-treated cells (Fig. 8F). A reduced level of chlorate (20 mM) was shown to exhibit similar effects, although to a lesser extent (data not shown). When TM cells were treated with *β*-xyloside, again fine fibronectin fibrils were reduced and thicker fibrils were observed (Fig. 8G). Tenascin C colocalized to

some of these thicker fibronectin fibrils, but it also immunostained discrete patches where fibronectin was not found (Fig. 8H, 8I). Cell staining with the viability–cytotoxicity kit for mammalian cells determined that none of the treatments caused significant cell death compared with that in the nontreated control cells (data not shown).

Discussion

This study was initiated to investigate further the role of GAG chains in outflow facility. The use of chemical GAG modifiers bypasses many criticisms of the earlier GAGase enzyme studies, such as differences in enzyme types, potential protease contaminations, potential to actually access the resistance molecules and digestion conditions. Changes were observed in both human and porcine eyes, and these results provide definitive evidence that GAGs play a role in outflow resistance in human eyes. The very different molecular mechanisms of these two inhibitors further strengthen this evidence.

Differences in response were observed between human and porcine anterior segments. An approximate 1.5-fold increase in outflow facility was induced in human eyes over a 120-hour treatment period (Fig. 5). This increase was comparable to the increase in outflow facility for human anterior segments treated with MMPs or IL-1α.[34] However, porcine eyes responded somewhat differently, as response time was faster, and the maximum increase in outflow facility was doubled (~3.5-fold) compared with human eyes (Fig. 2). In H&E stained histologic sections, it appeared that porcine TM contained significantly more cells than human TM (data not shown). In addition, human eyes used in this study were significantly older than porcine eyes, and they would have likely lost a substantial number of cells.[41,42] Older eyes would also be expected to have lower rates of cell metabolism. Thus, the reason that porcine eyes had a greater and faster response may be due to the fact that there were a larger number of healthier cells to respond to treatment. In addition, differences in molecular organization or configuration of the human and porcine outflow pathways may also contribute to differences in response.[31,43,44] An anomaly observed between species was that 50 mM chlorate increased outflow facility in human but not in porcine eyes (Figs. 2A, 5A). Histologic analysis of sections indicated that the TM beams in porcine eyes treated with 50 mM chlorate showed apparent compression (data not shown). Sulfated GAGs serving structural roles or providing intertrabecular charge repulsion, could account for the slight decrease in flow rate observed (Fig. 2).

Inhibition of GAG chain sulfation significantly reduced GAG chain immunostaining, but some sulfated GAG chain immunostaining remained after chlorate treatment (Figs. 3, 6). This staining may represent GAG chains that were deposited before treatment and that were not turned over during the experimental treatment time. However, chlorate competitively suppresses, but does not completely eliminate, sulfation of GAG chains,[24] and so some staining is not surprising. CS immunostaining in the JCT region of chlorate-treated eyes showed an intriguing striated appearance (Figs. 6B, 6E). The JCT region is the area where the outflow resistance is thought to reside,[10] making changes in the pattern of CS staining in this region particularly interesting. GAG chains may play a role in targeting proteoglycans to their specified extracellular place[5] and chondroitin-4 sulfation is crucial for localization of CS chains in cartilage.[45] Preliminary evidence indicates that expression of certain proteoglycans are disrupted in chlorate-treated TM (Keller KE et al. *IOVS* 2007;48:ARVO E-Abstract 2052) and suggests that GAG chain sulfation is critical for proper organization and composition of ECM in the JCT region. In addition, a recent study showed that mRNA levels of two sulfatase enzymes, extracellular sulfatase 1 (SULF1) and iduronate-2-sulfatase (IDS), are increased in POAG TM, whereas mRNA levels of a sulfotransferase, chondroitin-4-sulfotransferase 2 (CHST12), are decreased compared with that in normal TM.[46] A fine balance of sulfate group addition and removal must therefore exist to maintain GAG chain sulfation in vivo. Treatment

with chlorate disrupts this balance and leads to an increase in outflow facility. Manipulation of GAG chain sulfation may therefore be one mechanism by which TM cells can homeostatically adjust IOP. Although chlorate treatment can also reduce tyrosine sulfation in proteins,[47] the similar β-xyloside effect on outflow suggests that the outflow facility changes are more likely to be due to GAG's effects.

β-Xyloside was found to increase outflow within hours of initiation of treatment in the porcine eyes (Fig. 2A). At first, this seemed surprising, as the half-life of the average GAG chain in human eyes is approximately 36 hours.[48] However, the rate-limiting step in GAG biosynthesis is the activity of xylosyl transferase, which initiates the addition of a xylose monosaccharide onto specific serine residues of a core protein (Fig. 1).[49] β-xyloside treatment bypasses this rate-limiting step by diffusing into the cell and allowing direct addition of disaccharide units to it.[29] Therefore, GAG chain elongation can occur very quickly. After GAG chain elongation, it has been estimated that sulfation and translocation of a completed HS chain to the cell surface occurs in 12 to 15 minutes.[50] In addition, β-xyloside increases synthesis rates of CS chains but not of HS chains.[3,29] These observations argue that the relatively rapid increase in outflow facility of β-xyloside-treated anterior segments might have been expected. In addition, there are likely multiple pools of GAG chains in TM. In cartilage, there are two pools: one with a rapid turnover rate and one with a much slower rate.[51] If two or more pools do exist in the TM, β-xyloside probably replaces the rapidly turned over GAG chain population.

Once secreted into the ECM, free β-xyloside GAG chains may also disrupt protein–GAG interactions in the ECM by directly competing for GAG-binding motifs. For example, versican binds to the cell adhesion molecule CD44 via its CS chains and to HA via its amino-terminal region.[52] β-Xyloside could disrupt versican-CD44 binding, which would have downstream effects on cell adhesion, because this interaction is thought to stabilize HA–versican interactions at the cell surface.[52] In addition, the HepII domain of fibronectin has at least two sites for interaction with HS GAGs, whereas the alternatively spliced IIICS region can contribute an additional GAG-binding site.[32,53] Therefore, β-xyloside could abrogate fibronectin interactions with syndecans, a family of HS-containing, HepII-binding proteoglycans.[54] Interestingly, a recombinant HepII domain has been perfused into human anterior segments and found to increase outflow facility.[55] GAG chains also bind cytokines and growth factors.[27,56,57] These examples represent just a few of a plethora of potential protein-GAG interactions that could be affected by β-xyloside and chlorate treatments.

Previous studies have suggested that there is segmental variation around an eye, and the thickness of the JCT region in human eyes was found to vary up to 35% circumferentially.[58] Further, there are segmental flow differences throughout the TM.[59,60] Here, TM tissue from around the whole eye was analyzed by cutting each eye into 8 to 10 wedges and embedding them all into a single paraffin block. Sections from all the wedges were then analyzed by immunofluorescence, giving a global perspective of immunostaining in each eye. Staining with GAG antibodies in humans, and especially with HA-binding protein, was found to be somewhat variable between different wedges of the eye. The images presented are representative of at least three eyes per treatment and what was deemed to be the most consistent staining pattern observed for each antibody. It is attractive to think that the variability in the pattern of GAG chain staining correlates with areas of increased or decreased flow. However, we have no conclusive evidence of this assumption yet. Even though HA-binding protein staining was variable, there was decreased staining in chlorate- and β-xyloside-treated anterior segments (Figs. 6J–L). HA is not sulfated and does not attach to a core protein and so would not be directly affected by either of the treatments investigated. This fact suggests that disruption of other types of GAG chains leads to an indirect loss of HA. Localization of KS GAG chains was not determined, as KS chains are a relatively minor component of the total GAG population in the TM[61] and are N-linked to a core protein and so are not affected by β-xyloside treatment.

[30,62] However, there remains a possibility that KS-bearing proteoglycans are also indirectly affected.

Treatment with GAGases to specifically degrade GAG chains in porcine anterior perfusion culture showed that chondroitinase ABC had the greatest effect on outflow, compared with heparitinase or hyaluronidase (Fig. 4). Of interest, CS chains have been found to accumulate in the JCT of POAG eyes,[7] suggesting that CS may be important in regulation of aqueous outflow. When all three GAGase enzymes were combined, there was a faster and greater increase in outflow facility. Degradation of one type of GAG chain may allow greater access for the other GAGases. For example, degradation of HA with hyaluronidase may allow chondroitinase ABC greater access to CS/DS chains. The effect of GAG biosynthesis inhibitors on HA (Fig. 6J–L) also suggests that interactions between GAG types is necessary for the structural organization of outflow resistance. Human eyes treated with the same enzymes, and similar conditions as described for the pig, did not exhibit increased outflow facility (data not shown). This is contradictory with a report showing an increase in outflow facility when human eyes were treated with heparitinase (Johnson DH, et al. *IOVS* 1999;40:ARVO Abstract 504). However, differences of time and the magnitude of response between human and porcine eyes for chlorate and β-xyloside treatments suggest that further variations in GAGase treatment conditions may facilitate a response in human eyes.

Fibronectin assembly is a multistep process that is initiated when compact, soluble fibronectin is secreted and binds to the cell surface integrin $\alpha 5\beta 1$.[63] Initially, short fibrils are assembled around the cell periphery, but soluble fibronectin is incorporated, and larger, thicker fibrils form in a hierarchical process.[64] Both fine and thicker fibronectin fibrils were observed in nontreated human TM cells in culture, but a network of fine fibrils predominated (Fig. 8A). Both 50 mM chlorate and, to a lesser extent, β-xyloside treatment led to an increased number of thick fibronectin fibrils (Figs. 8D, 8G), suggesting a role for GAG chains in fibronectin fibril assembly. Fibronectin fibrils of mutant CHO cells exhibiting reduced N- and O-sulfation were found to be longer and thicker, with extensive branching compared to fibronectin in normal CHO cells.[65] This pattern is similar to our results with cells treated with chlorate, the inhibitor of sulfation. Fibronectin expression in β-xyloside-treated tissue was also found to differ. In control eyes, fibronectin was found throughout the beams, whereas in treated eyes, there was strong labeling at beam edges accompanied by a loss of central beam labeling (Fig. 7). Production of thicker fibronectin fibrils, as observed in cell culture, could account for the more intense edge staining, which correlates to where TM cells reside.

Binding of tenascin C to fibronectin in vitro has been demonstrated.[66] Tenascin C binding to fibronectin fibrils was stronger than to purified soluble fibronectin, suggesting that some other ECM component was involved in this interaction.[65] In baby hamster kidney (BHK) cells, tenascin C was colocalized to thick, well-developed fibronectin fibrils, whereas fine fibrils were not stained.[65,67] This pattern of staining was generally observed in TM cells, although in nontreated cells, there were also discrete patches of tenascin C staining in areas without fibronectin staining (Fig. 8C). In chlorate and β-xyloside-treated cells, tenascin C became colocalized to thick fibronectin fibrils (Figs. 8F, 8I). Enhanced incorporation of tenascin C into thick fibronectin fibrils was also observed in the reduced-sulfation mutant CHO cells described above.[67] These observations suggest that undersulfation of GAGs causes fibronectin and tenascin C to interact. Consequently, binding of tenascin C to the HepII region would reduce cell adhesion by disrupting fibronectin binding to the cell via syndecan-4, abrogating cell signaling via the RhoA and FAK pathways.[68,69] Conversely, addition of exogenous GAGs inhibited tenascin C-fibronectin interactions in vitro.[67] Thus, it is likely that GAG chains normally function to mediate fibronectin-tenascin C interactions. In human TM, there is loss of sulfated GAGs during normal aging,[9] whereas there is an accumulation of CS GAG chains in POAG eyes.[7] The results in our study suggest that in normal aged eyes, fibronectin-tenascin

C interactions occur because of the lack of sufficient GAG chains and would therefore reduce cell adhesion. In POAG eyes, the increased number of CS chains could limit fibronectin-tenascin C interactions, inhibiting the antiadhesive function of tenascin C. Therefore, regulation of GAG chain numbers may be one mechanism by which TM cells normally act to alter their extracellular environment in eyes. Cells can modulate GAG chains by synthesizing altered amounts of proteoglycans or by introducing or deleting domains for GAG attachment by alternative splicing.[32,33]

The exact mechanism by which chlorate and β-xyloside treatment increases outflow facility is still unknown. It is likely that disruption of ECM structural integrity and interruption of normal protein-GAG interactions both contribute. However, these results present the first definitive evidence for a direct role of GAG chains in the regulation of outflow resistance in the human eye and for modulation of ECM composition and organization by manipulation of GAG chains in the TM. Minor changes in this finely tuned web of interactions are likely to adjust outflow resistance and modulate IOP in vivo.

Acknowledgements

The authors thank Ruth Phinney at the Lions Eye Bank for facilitating procurement of human eyes, Carolyn Gendron at the OHSU Cancer Center for paraffin-embedded sectioning and histology, Aurelie Snyder at the core facility of the OHSU Department of Molecular Microbiology and Immunology for help with confocal microscopy, and Genevieve Long, PhD, for editorial assistance.

Supported by National Institutes of Health Grants EY003279, EY008247, and EY010572, Collins Medical Trust (Portland, OR), and by an unrestricted grant to the Casey Eye Institute from Research to Prevent Blindness (New York, NY).

References

1. Sasisekharan R, Raman R, Prabhakar V. Glycomics approach to structure-function relationships of glycosaminoglycans. Annu Rev Biomed Eng 2006;8:181–231. [PubMed: 16834555]
2. Davies JA, Fisher CE, Barnett MW. Glycosaminoglycans in the study of mammalian organ development. Biochem Soc Trans 2001;29:166–171. [PubMed: 11356147]
3. Silbert JE, Sugumaran G. Biosynthesis of chondroitin/dermatan sulfate. IUBMB Life 2002;54:177–186. [PubMed: 12512856]
4. Sugahara K, Kitagawa H. Heparin and heparan sulfate biosynthesis. IUBMB Life 2002;54:163–175. [PubMed: 12512855]
5. Prydz K, Dalen KT. Synthesis and sorting of proteoglycans. J Cell Sci 2000;113:193–205. [PubMed: 10633071]
6. Scott JE. Extracellular matrix, supramolecular organisation and shape. J Anat 1995;187:259–269. [PubMed: 7591990]
7. Knepper PA, Goossens W, Hvizd M, Palmberg PF. Glycosaminoglycans of the human trabecular meshwork in primary open-angle glaucoma. Invest Ophthalmol Vis Sci 1996;37:1360–1367. [PubMed: 8641839]
8. Tawara A, Varner HH, Hollyfield JG. Distribution and characterization of sulfated proteoglycans in the human trabecular tissue. Invest Ophthalmol Vis Sci 1989;30:2215–2231. [PubMed: 2793361]
9. Gong H, Freddo TF, Johnson M. Age-related changes of sulfated proteoglycans in the normal human trabecular meshwork. Exp Eye Res 1992;55:691–709. [PubMed: 1478279]
10. Johnson M. What controls aqueous humour outflow resistance? Exp Eye Res 2006;82:545–557. [PubMed: 16386733]
11. Francois J. The importance of the mucopolysaccharides in intraocular pressure regulation. Invest Ophthalmol 1975;14:173–176. [PubMed: 123231]
12. Knepper PA, Goossens W, Palmberg PF. Glycosaminoglycan stratification of the juxtacanalicular tissue in normal and primary open-angle glaucoma. Invest Ophthalmol Vis Sci 1996;37:2414–2425. [PubMed: 8933758]

13. Barany EH, Scotchbrook S. Influence of testicular hyaluronidase on the resistance to flow through the angle of the anterior chamber. Acta Physiol Scand 1954;30:240–248. [PubMed: 13158098]
14. Peterson WS, Jocson VL. Hyaluronidase effects on aqueous outflow resistance: quantitative and localizing studies in the rhesus monkey eye. Am J Ophthalmol 1974;77:573–577. [PubMed: 4206619]
15. Van Buskirk EM, Brett J. The canine eye: in vitro studies of the intraocular pressure and facility of aqueous outflow. Invest Ophthalmol Vis Sci 1978;17:373–377. [PubMed: 640785]
16. Gum GG, Samuelson DA, Gelatt KN. Effect of hyaluronidase on aqueous outflow resistance in normotensive and glaucomatous eyes of dogs. Am J Vet Res 1992;53:767–770. [PubMed: 1524304]
17. Knepper PA, Farbman AI, Telser AG. Exogenous hyaluronidases and degradation of hyaluronic acid in the rabbit eye. Invest Ophthalmol Vis Sci 1984;25:286–293. [PubMed: 6698747]
18. Sawaguchi S, Lam TT, Yue BY, Tso MOM. Effects of Glycosaminoglycan-degrading enzymes on bovine trabecular meshwork in organ culture. J Glaucoma 1993;2:80–86.
19. Sawaguchi S, Yue BY, Yeh P, Tso MO. Effects of intracameral injection of chondroitinase ABC in vivo. Arch Ophthalmol 1992;110:110–117. [PubMed: 1731702]
20. Hubbard WC, Johnson M, Gong H, et al. Intraocular pressure and outflow facility are unchanged following acute and chronic intracameral chondroitinase ABC and hyaluronidase in monkeys. Exp Eye Res 1997;65:177–190. [PubMed: 9268586]
21. Pedler C. The relationship of hyaluronidase to aqueous outflow resistance. Trans Ophthalmol Soc UK 1956;76:51–63.
22. Francois J, Rabaey M, Neetens A. Perfusion studies on the outflow of aqueous humor in human eyes. Arch Ophthalmol 1956;55:193–204.
23. Grant WM. Experimental aqueous perfusion in enucleated human eyes. Arch Ophthalmol 1963;69:783–801. [PubMed: 13949877]
24. Greve H, Cully Z, Blumberg P, Kresse H. Influence of chlorate on proteoglycan biosynthesis by cultured human fibroblasts. J Biol Chem 1988;263:12886–12892. [PubMed: 3417641]
25. Klaassen CD, Boles JW. Sulfation and sulfotransferases 5: the importance of 3′-phosphoadenosine 5′-phosphosulfate (PAPS) in the regulation of sulfation. FASEB J 1997;11:404–418. [PubMed: 9194521]
26. Safaiyan F, Kolset SO, Prydz K, Gottfridsson E, Lindahl U, Salmivirta M. Selective effects of sodium chlorate treatment on the sulfation of heparan sulfate. J Biol Chem 1999;274:36267–36273. [PubMed: 10593915]
27. Gorsi B, Stringer SE. Tinkering with heparan sulfate sulfation to steer development. Trends Cell Biol 2007;17:173–177. [PubMed: 17320398]
28. Kusche-Gullberg M, Kjellen L. Sulfotransferases in glycosaminoglycan biosynthesis. Curr Opin Struct Biol 2003;13:605–611. [PubMed: 14568616]
29. Schwartz NB, Galligani L, Ho PL, Dorfman A. Stimulation of synthesis of free chondroitin sulfate chains by beta-D-xylosides in cultured cells. Proc Natl Acad Sci USA 1974;71:4047–4051. [PubMed: 4372604]
30. Hahn RA, Birk DE. beta-D xyloside alters dermatan sulfate proteoglycan synthesis and the organization of the developing avian corneal stroma. Development 1992;115:383–393. [PubMed: 1425332]
31. Bachmann B, Birke M, Kook D, Eichhorn M, Lütjen-Drecoll E. Ultrastructural and biochemical evaluation of the porcine anterior chamber perfusion model. Invest Ophthalmol Vis Sci 2006;47:2011–2020. [PubMed: 16639010]
32. Vittal V, Rose A, Gregory KE, Kelley MJ, Acott TS. Changes in gene expression by trabecular meshwork cells in response to mechanical stretching. Invest Ophthalmol Vis Sci 2005;46:2857–2868. [PubMed: 16043860]
33. Keller KE, Kelley MJ, Acott TS. Extracellular matrix gene alternative splicing by trabecular meshwork cells in response to mechanical stretching. Invest Ophthalmol Vis Sci 2007;48:1164–1172. [PubMed: 17325160]
34. Bradley JM, Vranka J, Colvis CM, et al. Effect of matrix metalloproteinases activity on outflow in perfused human organ culture. Invest Ophthalmol Vis Sci 1998;39:2649–2658. [PubMed: 9856774]

35. Bradley JM, Anderssohn AM, Colvis CM, et al. Mediation of laser trabeculoplasty-induced matrix metalloproteinase expression by IL-1β and TNFα. Invest Ophthalmol Vis Sci 2000;41:422–430. [PubMed: 10670472]
36. Kelley MJ, Rose AY, Song K, et al. Synergism of TNF and IL-1 in the induction of matrix metalloproteinase-3 in trabecular meshwork. Invest Ophthalmol Vis Sci 2007;48:2634–2643. [PubMed: 17525194]
37. Morris NP, Oxford JT, Davies GB, Smoody BF, Keene DR. Developmentally regulated alternative splicing of the alpha1(XI) collagen chain: spatial and temporal segregation of isoforms in the cartilage of fetal rat long bones. J Histochem Cytochem 2000;48:725–741. [PubMed: 10820146]
38. Stamer WD, Seftor RE, Williams SK, Samaha HA, Snyder RW. Isolation and culture of human trabecular meshwork cells by extracellular matrix digestion. Curr Eye Res 1995;14:611–617. [PubMed: 7587308]
39. Polansky JR, Weinreb RN, Baxter JD, Alvarado J. Human trabecular cells. I. Establishment in tissue culture and growth characteristics. Invest Ophthalmol Vis Sci 1979;18:1043–1049. [PubMed: 383640]
40. Alexander JP, Samples JR, Van Buskirk EM, Acott TS. Expression of matrix metalloproteinases and inhibitor by human trabecular meshwork. Invest Ophthalmol Vis Sci 1991;32:172–180. [PubMed: 1846130]
41. Grierson I, Howes RC. Age-related depletion of the cell population in the human trabecular meshwork. Eye 1987;1:204–210. [PubMed: 3653434]
42. Alvarado J, Murphy C, Polansky J, Juster R. Age-related changes in trabecular meshwork cellularity. Invest Ophthalmol Vis Sci 1981;21:714–727. [PubMed: 7298275]
43. May CA, Skorski LM, Lütjen-Drecoll E. Innervation of the porcine ciliary muscle and outflow region. J Anat 2005;206:231–236. [PubMed: 15733294]
44. McMenamin PG, Steptoe RJ. Normal anatomy of the aqueous humour outflow system in the domestic pig eye. J Anat 1991;178:65–77. [PubMed: 1810936]
45. Kluppel M, Wight TN, Chan C, Hinek A, Wrana JL. Maintenance of chondroitin sulfation balance by chondroitin-4-sulfotransferase 1 is required for chondrocyte development and growth factor signaling during cartilage morphogenesis. Development 2005;132:3989–4003. [PubMed: 16079159]
46. Diskin S, Kumar J, Cao Z, et al. Detection of differentially expressed glycogenes in trabecular meshwork of eyes with primary open-angle glaucoma. Invest Ophthalmol Vis Sci 2006;47:1491–1499. [PubMed: 16565384]
47. Baeuerle PA, Huttner WB. Chlorate: a potent inhibitor of protein sulfation in intact cells. Biochem Biophys Res Commun 1986;141:870–877. [PubMed: 3026396]
48. Acott TS, Kingsley PD, Samples JR, Van Buskirk EM. Human trabecular meshwork organ culture: morphology and glycosaminoglycan synthesis. Invest Ophthalmol Vis Sci 1988;29:90–100. [PubMed: 3335436]
49. Kresse H, Seidler DG, Muller M, et al. Different usage of the glycosaminoglycan attachment sites of biglycan. J Biol Chem 2001;276:13411–13416. [PubMed: 11145959]
50. Yanagishita M, Hascall VC. Cell surface heparan sulfate proteoglycans. J Biol Chem 1992;267:9451–9454. [PubMed: 1577788]
51. Heinegard, D.; Paulsson, M. Structure and metabolism of proteoglycans. In: Piez, KA.; Reddi, AH., editors. Extracellular Matrix Biochemistry. New York: Elsevier Science; 1984. p. 277-328.
52. Wight TN. Versican: a versatile extracellular matrix proteoglycan in cell biology. Curr Opin Cell Biol 2002;14:617–623. [PubMed: 12231358]
53. Santas AJ, Peterson JA, Halbleib JL, Craig SE, Humphries MJ, Peters DM. Alternative splicing of the IIICS domain in fibronectin governs the role of the heparin II domain in fibrillogenesis and cell spreading. J Biol Chem 2002;277:13650–13658. [PubMed: 11832485]
54. Filla MS, David G, Weinreb RN, Kaufman PL, Peters DM. Distribution of syndecans 1–4 within the anterior segment of the human eye: expression of a variant syndecan-3 and matrix-associated syndecan-2. Exp Eye Res 2004;79:61–74. [PubMed: 15183101]
55. Santas AJ, Bahler C, Peterson JA, et al. Effect of heparin II domain of fibronectin on aqueous outflow in cultured anterior segments of human eyes. Invest Ophthalmol Vis Sci 2003;44:4796–4804. [PubMed: 14578401]

56. Bishop JR, Schuksz M, Esko JD. Heparan sulphate proteoglycans fine-tune mammalian physiology. Nature 2007;446:1030–1037. [PubMed: 17460664]
57. Deepa SS, Yamada S, Zako M, Goldberger O, Sugahara K. Chondroitin sulfate chains on syndecan-1 and syndecan-4 from normal murine mammary gland epithelial cells are structurally and functionally distinct and cooperate with heparan sulfate chains to bind growth factors. J Biol Chem 2004;279:37368–37376. [PubMed: 15226297]
58. Buller C, Johnson D. Segmental variability of the trabecular meshwork in normal and glaucomatous eyes. Invest Ophthalmol Vis Sci 1994;35:3841–3851. [PubMed: 7928181]
59. Ethier CR, Chan DW. Cationic ferritin changes outflow facility in human eyes whereas anionic ferritin does not. Invest Ophthalmol Vis Sci 2001;42:1795–1802. [PubMed: 11431444]
60. Hann CR, Bahler CK, Johnson DH. Cationic ferritin and segmental flow through the trabecular meshwork. Invest Ophthalmol Vis Sci 2005;46:1–7. [PubMed: 15623746]
61. Acott TS, Westcott M, Passo MS, Van Buskirk EM. Trabecular meshwork glycosaminoglycans in human and cynomolgus monkey eye. Invest Ophthalmol Vis Sci 1985;26:1320–1329. [PubMed: 4044160]
62. Funderburgh JL. Keratan sulfate biosynthesis. IUBMB Life 2002;54:187–194. [PubMed: 12512857]
63. Mao Y, Schwarzbauer JE. Fibronectin fibrillogenesis, a cell-mediated matrix assembly process. Matrix Biol 2005;24:389–399. [PubMed: 16061370]
64. Dallas SL, Chen Q, Sivakumar P. Dynamics of assembly and reorganization of extracellular matrix proteins. Curr Top Dev Biol 2006;75:1–24. [PubMed: 16984808]
65. Chung CY, Zardi L, Erickson HP. Binding of tenascin-C to soluble fibronectin and matrix fibrils. J Biol Chem 1995;270:29012–29017. [PubMed: 7499434]
66. Chiquet-Ehrismann R, Kalla P, Pearson CA, Beck K, Chiquet M. Tenascin interferes with fibronectin action. Cell 1988;53:383–390. [PubMed: 2452695]
67. Chung CY, Erickson HP. Glycosaminoglycans modulate fibronectin matrix assembly and are essential for matrix incorporation of tenascin-C. J Cell Sci 1997;110:1413–1419. [PubMed: 9217327]
68. Midwood KS, Valenick LV, Hsia HC, Schwarzbauer JE. Coregulation of fibronectin signaling and matrix contraction by tenascin-C and syndecan-4. Mol Biol Cell 2004;15:5670–5677. [PubMed: 15483051]
69. Huang W, Chiquet-Ehrismann R, Moyano JV, Garcia-Pardo A, Orend G. Interference of tenascin-C with syndecan-4 binding to fibronectin blocks cell adhesion and stimulates tumor cell proliferation. Cancer Res 2001;61:8586–8594. [PubMed: 11731446]

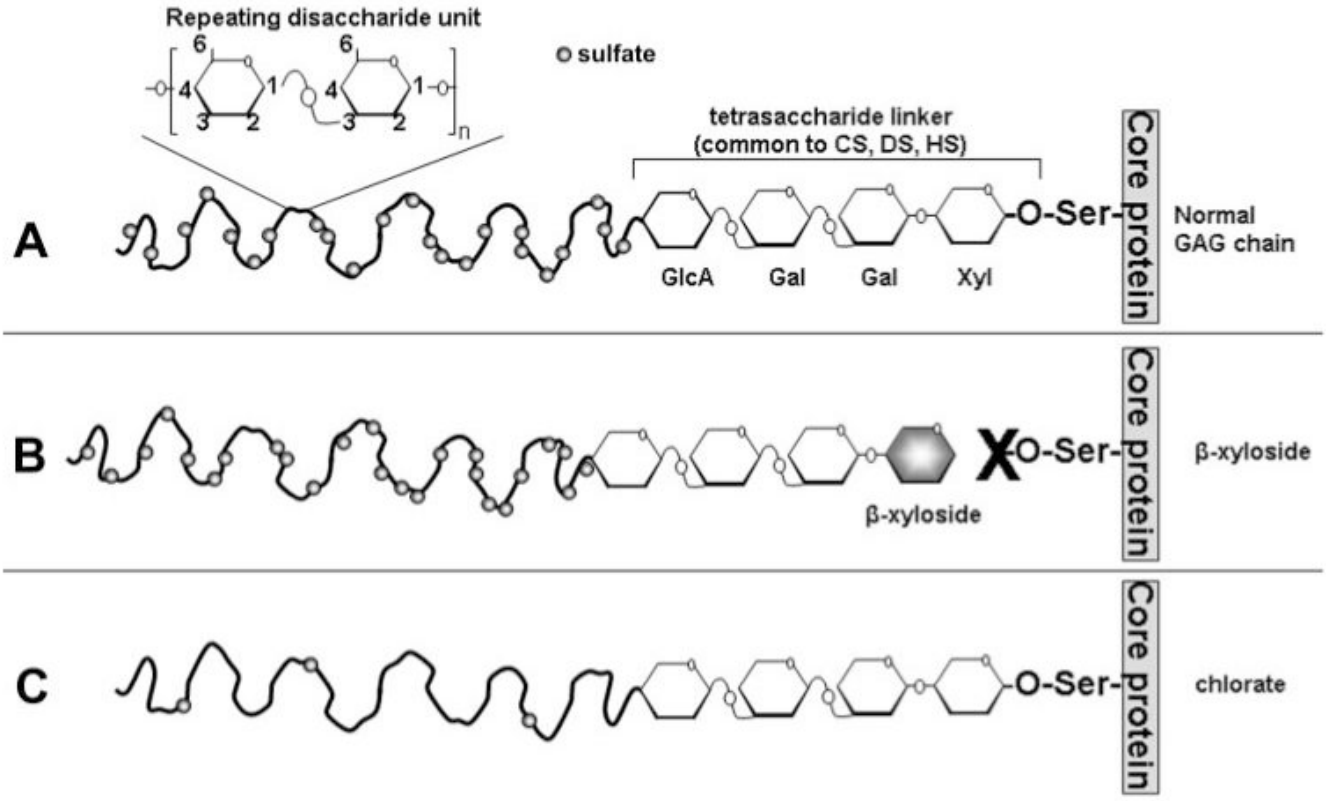

Figure 1.

GAG chain biosynthesis. (**A**) GAG chains of CS, DS, and HS are O-linked to a serine (Ser) residue of a core protein as it passes through the endoplasmic reticulum. GAG chain elongation is initiated by the addition of 4 monosaccharide residues (xylose [Xyl], galactose [Gal], galactose, and glucuronic acid [GlcA]). To this linker region, repeating GAG-specific disaccharide units are added. A Glc-NAc (*N*-acetyl-glucosamine) residue is added next for heparan sulfate chains, and a GalNAc (*N*-acetyl-galactosamine) residue is added next for CS/DS chains. GAG chains are subsequently sulfated (*circles*) before secretion. For CS chains, sulfation can occur at the 4- or 6-hydroxyl positions; for DS, sulfation can occur at the 2- or 4-hydroxyl positions; for HS, sulfation can occur at the *N*-, 2-, 3- or 6-hydroxyl positions. (**B**) *β*-Xyloside acts as a nucleation point on which disaccharide units can be added instead of on the core protein. This competitively inhibits GAG attachment to the proteoglycan. (**C**) Sodium chlorate acts as a sulfate inhibitor. Although GAG chain attachment to the core protein and chain elongation occur normally, the resultant GAG chain is highly undersulfated.

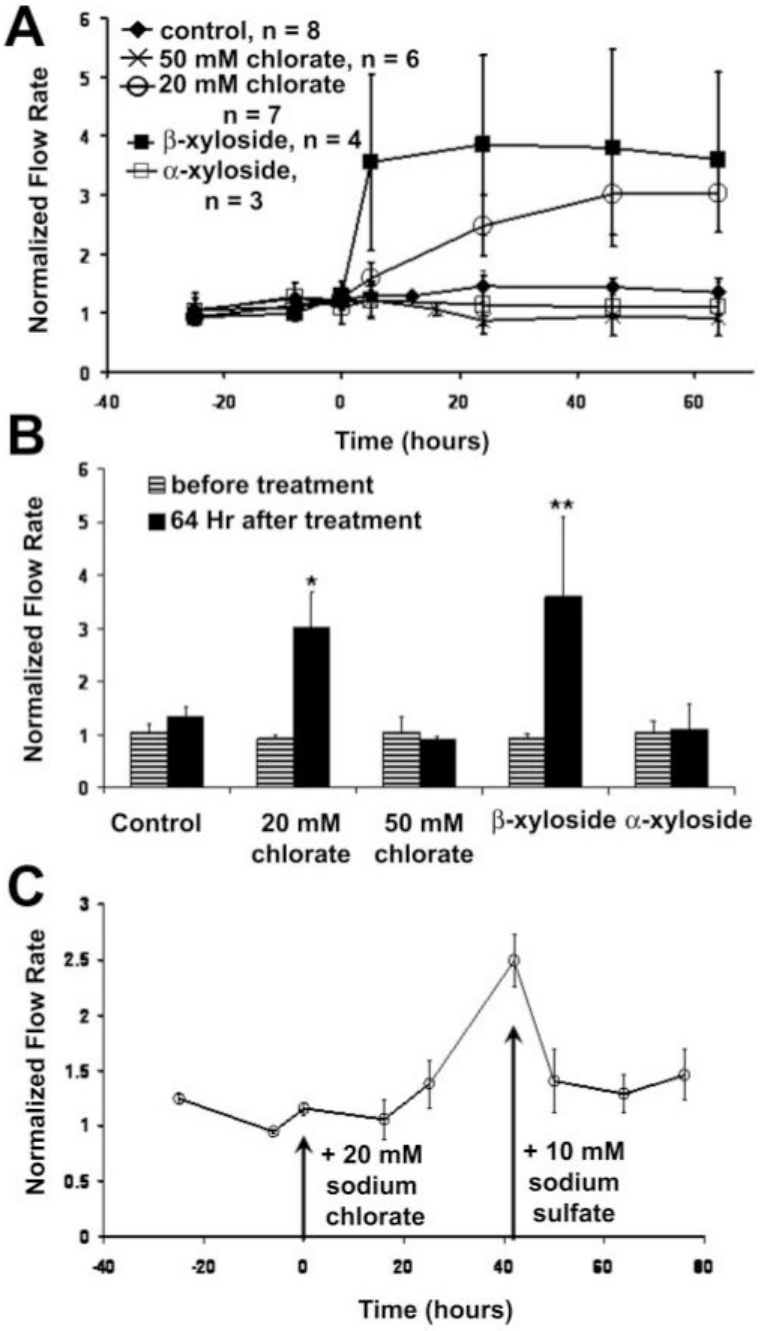

Figure 2.

Effects of chlorate and *β*-xyloside on outflow facility in porcine eyes. (**A**) Porcine anterior segments were perfused with 20 mM or 50 mM sodium chlorate, or 1 mM *α*- or *β*-xyloside. Data are expressed as the normalized flow, that is, flow at each time point/average flow before treatment. Time point 0 represents the start of treatment. The number of eyes used for each treatment is noted. Data are expressed as the mean ± SEM. (**B**) Facility data presented as normalized flow rate before treatment and 64 hours after treatment. A Mann-Whitney rank sum test was performed to compare flow rates before and after treatment; **P* = 0.001; ***P* = 0.029. (**C**) Addition of 10 mM sodium sulfate to the culture medium to reverse the effect of 20 mM chlorate treatment on outflow (*n* = 8). Data are expressed as the mean ± SEM.

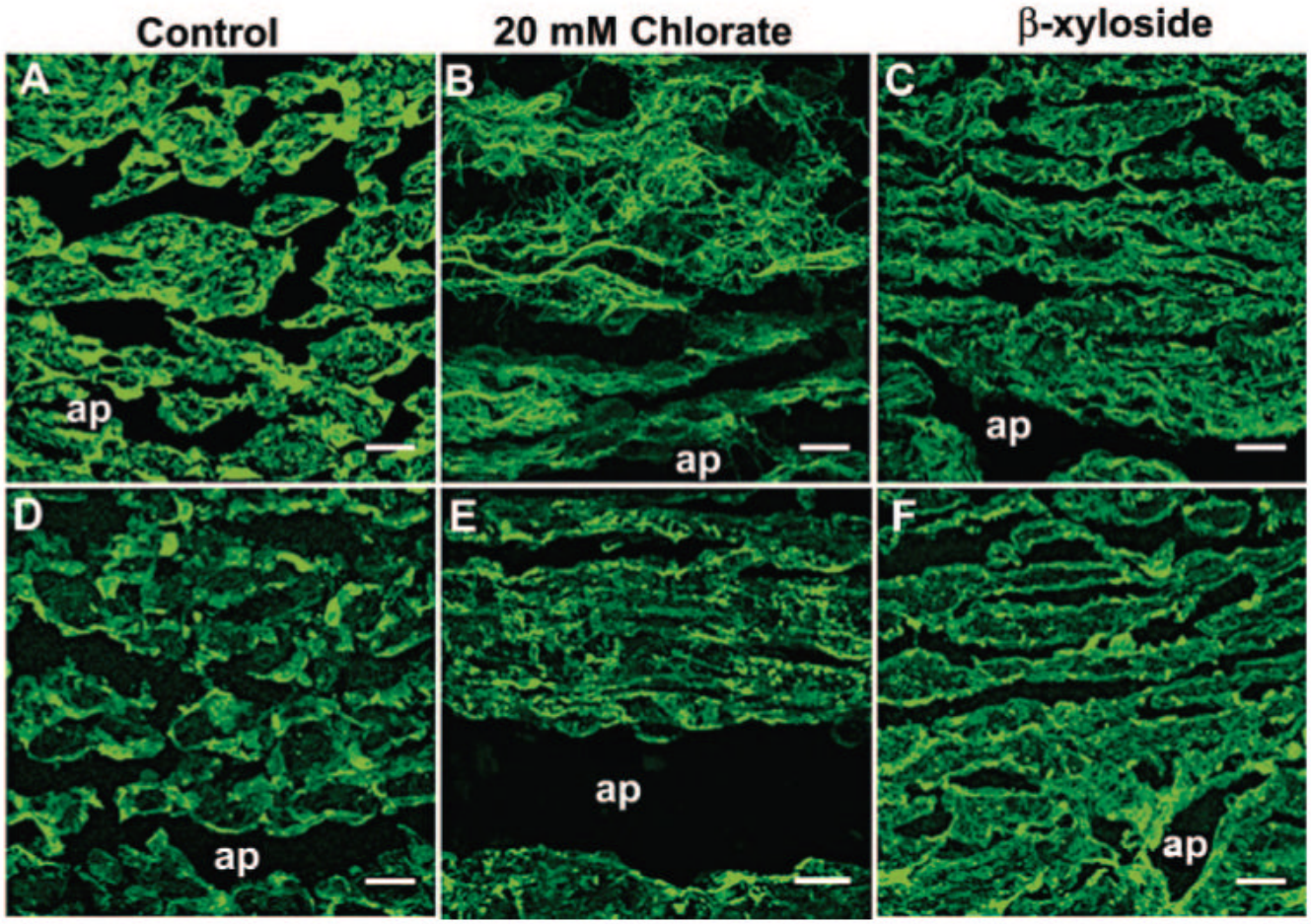

Figure 3.
Chondroitin sulfate immunostaining in the TM of chlorate-and β-xyloside-treated porcine eyes. The distribution of C4S (**A–C**) and C6S (**D–F**) was investigated in (**A, D**) control and (**B, E**) 20-mM chlorate- or (**C, F**) β-xyloside-perfused porcine anterior segments. ap, aqueous plexus. Scale bars, 10 μm.

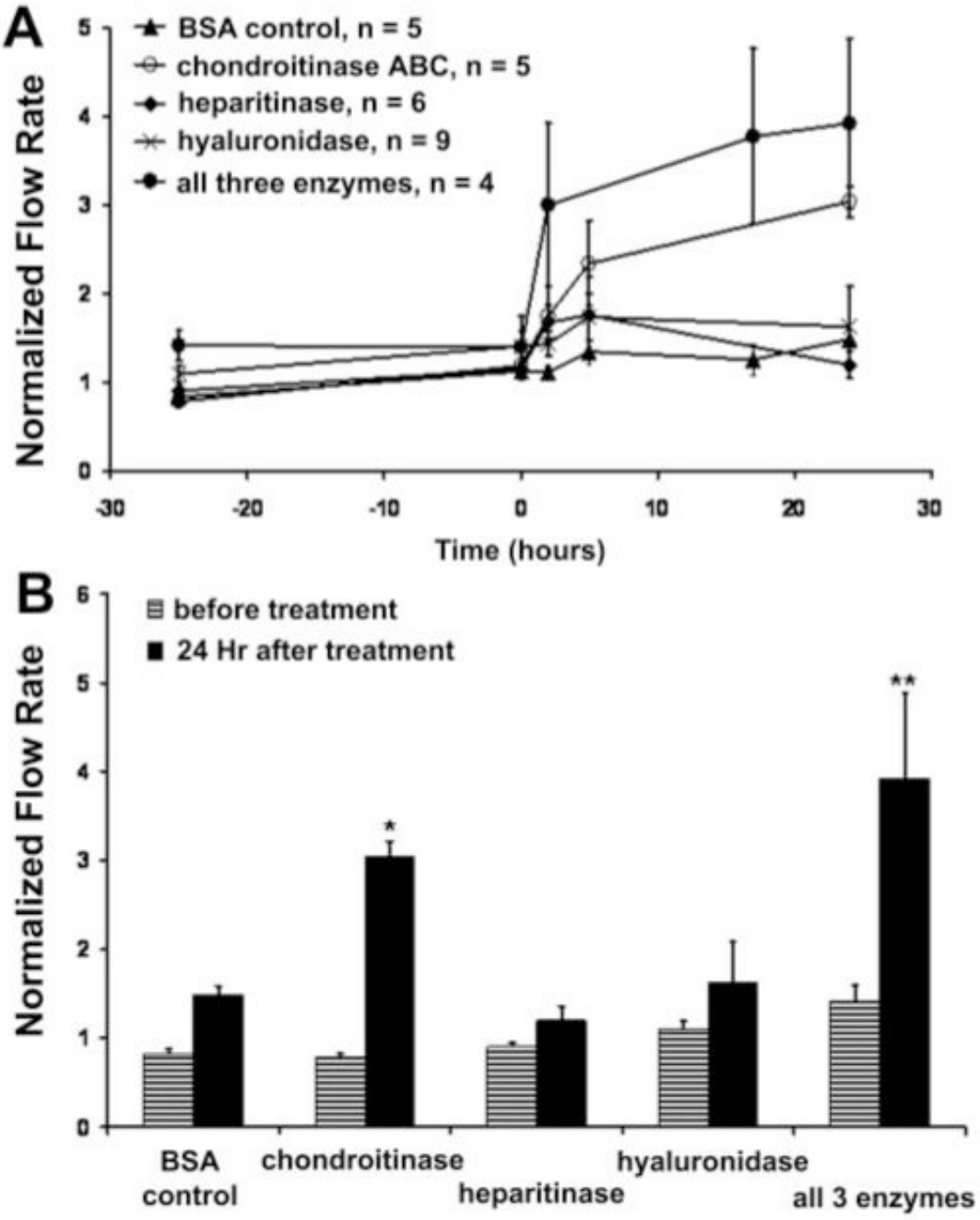

Figure 4.

Treatment of porcine anterior segments with GAGases. (**A**) Porcine anterior segments were treated in perfusion culture with chondroitinase ABC (0.25 U/mL), heparitinase (0.01 U/mL), or hyaluronidase (10 U/mL), individually or in combination. Control eyes were treated with 0.1% BSA in PBS. Time point 0 represents the start of treatment. Data are expressed as the mean ± SEM. (**B**) Facility data presented as normalized flow rates before treatment and 24 hours after GAGase treatment. A Mann-Whitney rank sum test was performed to compare flow rates before and after treatment; **P* < 0.001; ***P* = 0.029.

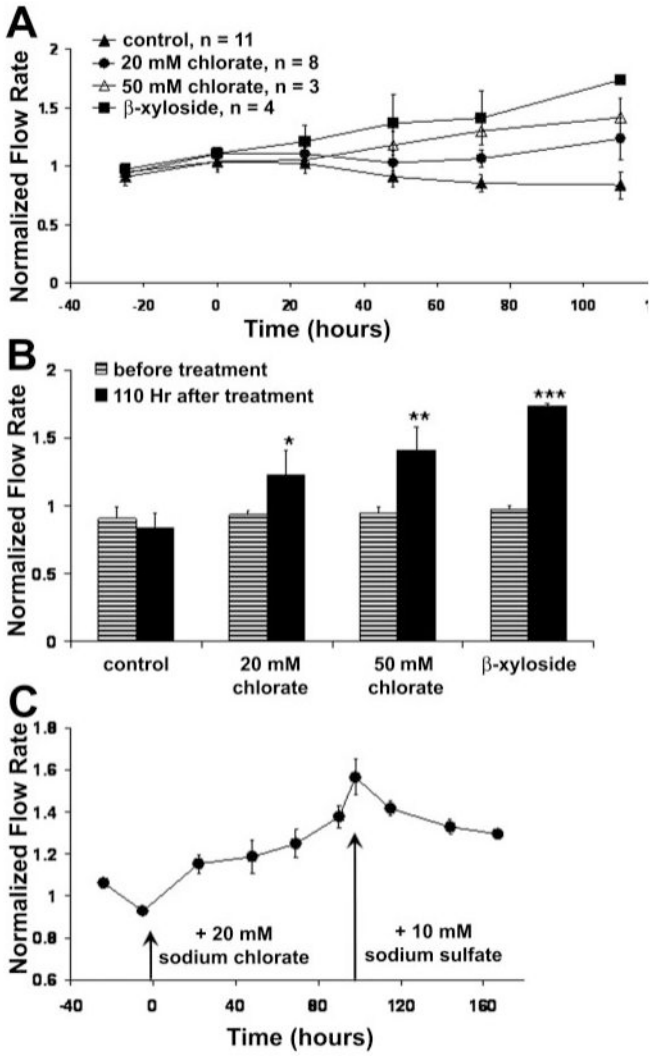

Figure 5.

Effects of chlorate and *β*-xyloside on outflow facility in human eyes. (**A**) Human anterior segments were perfused with 20 or 50 mM sodium chlorate or 1 mM *β*-xyloside. Data are expressed as the normalized flow. Time point 0 represents the start of treatment. Data are expressed as the mean ± SEM. (**B**) Facility data are presented as normalized flow rates before treatment and at 24 hours after GAGase treatment. A Student's *t*-test was performed to compare flow rates before and after treatment; **P* = 0.024; ***P* = 0.001; ****P* = 0.016. (**C**) Addition of 10 mM sodium sulfate to the culture medium reversed the effect of 20 mM chlorate treatment on outflow (*n* = 4). Data are expressed as the mean ± SEM.

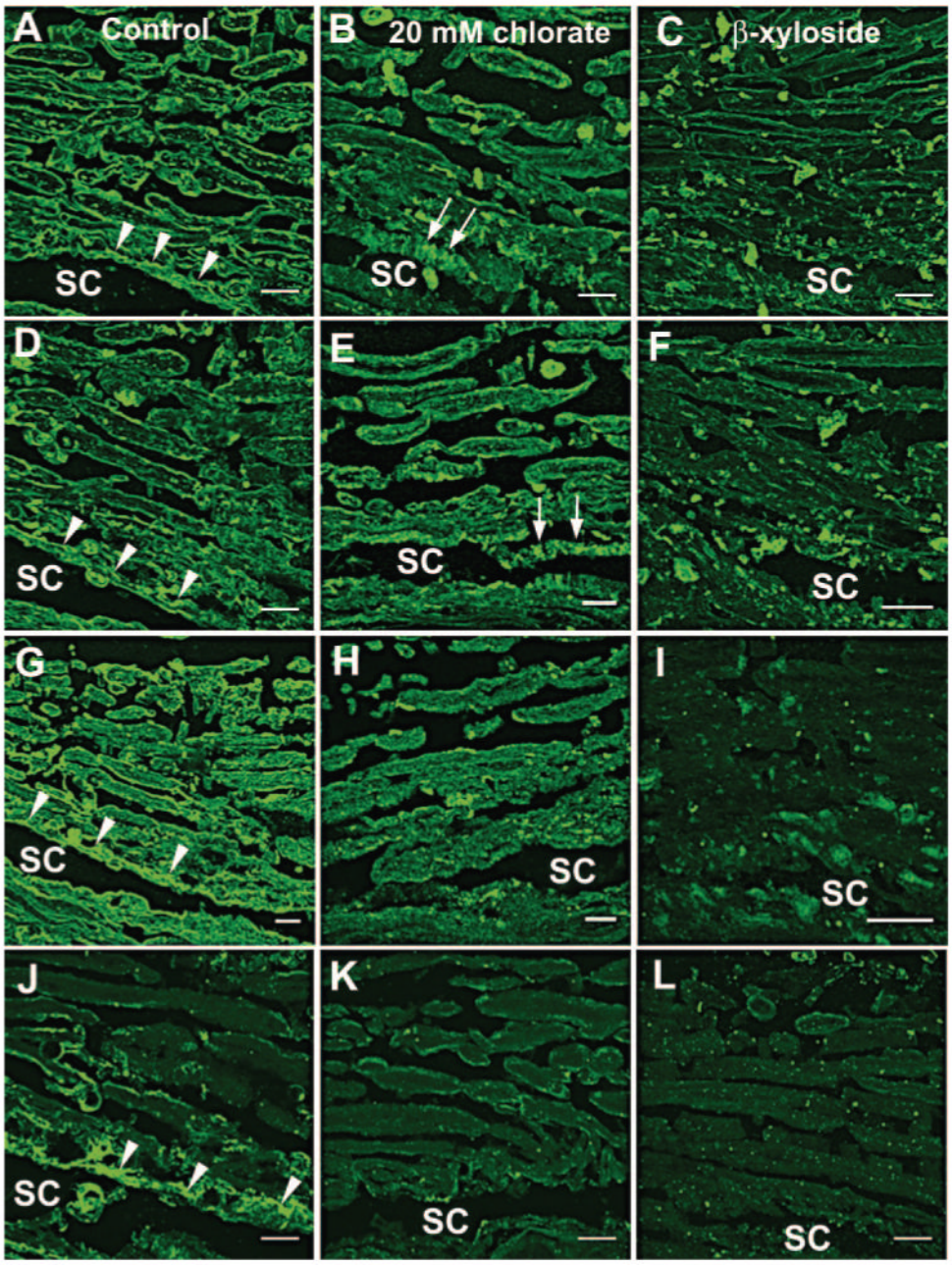

Figure 6.

Staining of GAG chains in human eyes after chlorate or *β*-xyloside treatment. Distributions of C4S (**A–C**), C6S (**D–F**), HS (**G–I**), and HA (**J–L**), detected by HA-binding protein, were investigated in (**A, D, G, J**) control, (**B, E, H, K**) 20-mM chlorate-, or (**C, F, I, L**) *β*-xyloside-perfused human eyes. For control and 20-mM chlorate-treated sections, the images shown are a pair of eyes from the same individual. *Arrowheads*: staining in the JCT region; *arrows*: apparent striations in the JCT region of chlorate-treated eyes (**B, E**). Images are representative of three pairs of eyes that were treated with 20 mM chlorate or *β*-xyloside. SC, Schlemm's canal. Scale bars, 10 *μ*m.

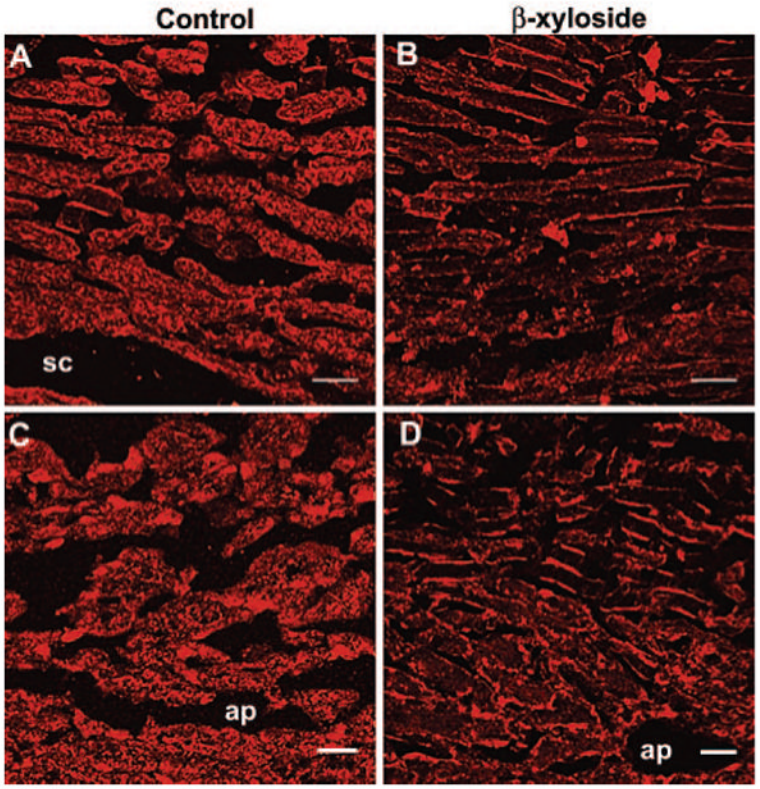

Figure 7.

Expression of fibronectin in control and β-xyloside-treated eyes. The distribution of fibronectin was investigated in (**A, C**) control and (**B, D**) β-xyloside-perfused (**A, B**) human or (**C, D**) porcine eyes. sc, Schlemm's canal; ap, aqueous plexus. Scale bars, 10 μm.

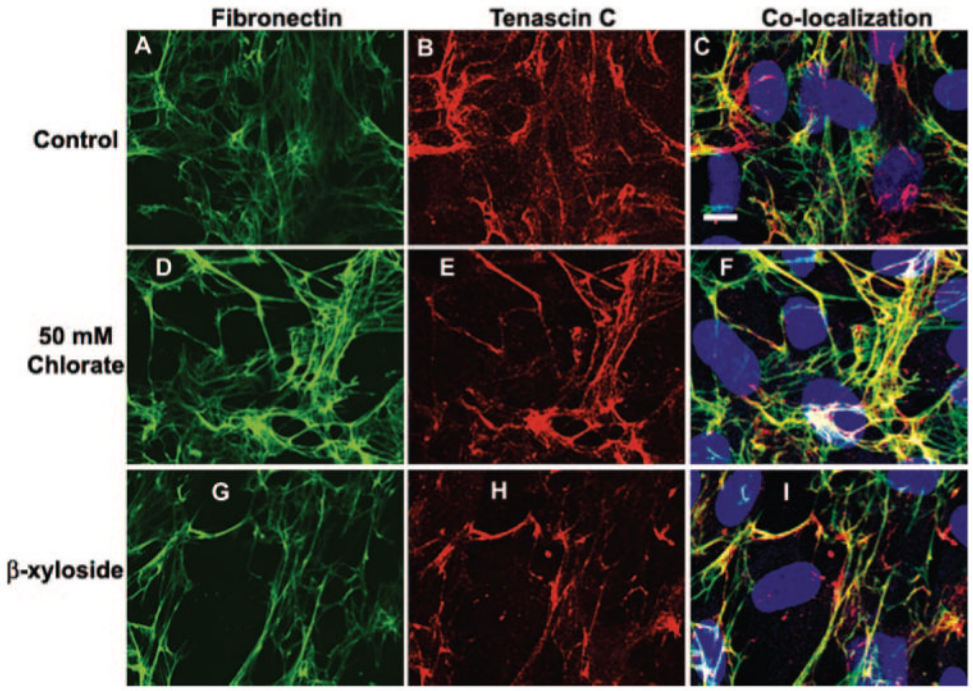

Figure 8.

Confocal microscopy of TM cells in culture. Human TM cells cultured in medium alone (**A–C**) or supplemented with 50 mM sodium chlorate (**D–F**) or *β*-xyloside (**G–I**) for 72 hours. Slides were fixed and immunostained with fibronectin and tenascin C antibodies and labeled with Draq5 nuclear stain. Scale bar, 10 *μ*m.

Table 1

Summary of Information and Flow Facility Data for Human Donor Eyes

Eye ID	Age (y)	Sex	Treatment	Before*	After*	Change (*x*-Fold)
2006-0681	88	F	OS, n/a	—	—	—
			OD, ctrl	4.38	4.67	1.066
2006-0682	92	F	OS, ctrl	1.89	1.81	0.957
			OD, 20 mM chlorate	5.8	6.46	1.113
2006-0683	90	F	OS, ctrl	5.66	5.76	1.017
			OD, 20 mM chlorate	3.18	4.14	1.302
2006-0694	77	F	OS, n/a	—	—	—
			OD, *β*-xyloside	2.01	3.38	1.682
2006-0707	89	M	OS, n/a	—	—	—
			OD, 50 mM chlorate	4.45	6.24	1.402
2006-0742	72	M	OS, n/a	—	—	—
			OD, 20 mM chlorate	1.29	1.32	1.023
2006-0797	80	M	OS, n/a	—	—	—
			OD, ctrl	1.32	1.12	0.848
2006-0808	87	M	OS, 20 mM chlorate	1.95	2.00	1.025
			OD, ctrl	6.55	6.83	1.043
2006-1074	74	M	OS, 20 mM chlorate	5.02	6.04	1.203
			OD, n/a	—	—	—
2007-0118	78	M	OS, ctrl	2.18	1.25	0.573
			OD, 20 mM chlorate	3.3	2.6	0.787
2007-0123	100	F	OS, 20 mM chlorate	1.39	1.52	1.093
			OD, ctrl	2.8	1.64	0.585
2007-0233	83	M	OS, 50 mM chlorate	0.94	1.088	1.157
			OD, ctrl	2.04	1.18	0.578
2007-0347	47	M	OS, 20 mM chlorate	1.92	4.18	2.177
			OD, ctrl	1.91	1.94	1.015
2007-0348	68	M	OS, 50 mM chlorate	1.63	2.814	1.726
			OD, ctrl	2.81	3.07	1.092
2007-0358	75	M	OS, ctrl	2.46	2.91	1.183

Eye ID	Age (y)	Sex	Treatment	Before*	After*	Change (*x*-Fold)
			OD, *β*-xyloside	1.66	2.46	1.481
2007-0379	76	M	OS, n/a	—	—	—
			OD, *β*-xyloside	4.14	7.22	1.744
2007-0990	92	F	OS, 50 mM chlorate	4.27	8.454	1.979
			OD, 50 mM chlorate	1.18	1.46	1.237
2007-1020	74	F	OS, 50 mM chlorate	1.45	1.988	1.371
			OD, n/a	—	—	—

*Average flow rates in microliters per minute before and after treatments.